



RESEARCH

Open Access



Mutations in ALK signaling pathways conferring resistance to ALK inhibitor treatment lead to collateral vulnerabilities in neuroblastoma cells

Mareike Berlak^{1,2,3†} , Elizabeth Tucker^{4†}, Mathurin Dorel^{5,6,7}, Annika Winkler¹, Aleixandria McGearey¹, Elias Rodriguez-Fos^{1,8}, Barbara Martins da Costa⁴, Karen Barker⁴, Elicia Fyle⁴, Elizabeth Calton⁴, Selma Eising⁹, Kim Ober⁹, Deborah Hughes¹⁰, Eleni Koutroumanidou¹⁰, Paul Carter¹⁰, Reda Stankunaite¹⁰, Paula Proszek¹⁰, Neha Jain¹¹, Carolina Rosswog¹², Heathcliff Dorado-Garcia¹, Jan Jasper Molenaar^{9,13}, Mike Hubank¹⁰, Giuseppe Barone¹¹, John Anderson¹¹, Peter Lang^{1,14}, Hedwig Elisabeth Deubzer^{1,8,15,16}, Annette Künkele^{1,15,16,17}, Matthias Fischer¹², Angelika Eggert^{1,15,16,17}, Charlotte Kloft³, Anton George Henssen^{1,8,15,16,17}, Michael Boettcher¹⁸, Falk Hertwig¹, Nils Blüthgen^{6,7,15,16,17}, Louis Chesler^{4†} and Johannes Hubertus Schulte^{1,15,16*†} 

Abstract

Background: Development of resistance to targeted therapies has tempered initial optimism that precision oncology would improve poor outcomes for cancer patients. Resistance mechanisms, however, can also confer new resistance-specific vulnerabilities, termed collateral sensitivities. Here we investigated anaplastic lymphoma kinase (ALK) inhibitor resistance in neuroblastoma, a childhood cancer frequently affected by activating ALK alterations.

Methods: Genome-wide forward genetic CRISPR-Cas9 based screens were performed to identify genes associated with ALK inhibitor resistance in neuroblastoma cell lines. Furthermore, the neuroblastoma cell line NBLW-R was rendered resistant by continuous exposure to ALK inhibitors. Genes identified to be associated with ALK inhibitor resistance were further investigated by generating suitable cell line models. In addition, tumor and liquid biopsy samples of four patients with *ALK*-mutated neuroblastomas before ALK inhibitor treatment and during tumor progression under treatment were genomically profiled.

Results: Both genome-wide CRISPR-Cas9-based screens and preclinical spontaneous ALKi resistance models identified *NF1* loss and activating *NRAS*^{Q61K} mutations to confer resistance to chemically diverse ALKi. Moreover, human neuroblastomas recurrently developed de novo loss of *NF1* and activating RAS mutations after ALKi treatment, leading to therapy resistance. Pathway-specific perturbations confirmed that *NF1* loss and activating RAS mutations lead

†Mareike Berlak, Elizabeth Tucker, Louis Chesler and Johannes H. Schulte contributed equally to this work.

*Correspondence: Johannes.schulte@charite.de

¹ Department of Pediatric Oncology/Hematology, Charité – Universitätsmedizin Berlin, Augustenburger Platz 1, 13353 Berlin, Germany
Full list of author information is available at the end of the article



© The Author(s) 2022. **Open Access** This article is licensed under a Creative Commons Attribution 4.0 International License, which permits use, sharing, adaptation, distribution and reproduction in any medium or format, as long as you give appropriate credit to the original author(s) and the source, provide a link to the Creative Commons licence, and indicate if changes were made. The images or other third party material in this article are included in the article's Creative Commons licence, unless indicated otherwise in a credit line to the material. If material is not included in the article's Creative Commons licence and your intended use is not permitted by statutory regulation or exceeds the permitted use, you will need to obtain permission directly from the copyright holder. To view a copy of this licence, visit <http://creativecommons.org/licenses/by/4.0/>. The Creative Commons Public Domain Dedication waiver (<http://creativecommons.org/publicdomain/zero/1.0/>) applies to the data made available in this article, unless otherwise stated in a credit line to the data.

to RAS-MAPK signaling even in the presence of ALKi. Intriguingly, *NF1* loss rendered neuroblastoma cells hypersensitive to MEK inhibition.

Conclusions: Our results provide a clinically relevant mechanistic model of ALKi resistance in neuroblastoma and highlight new clinically actionable collateral sensitivities in resistant cells.

Keywords: Neuroblastoma, CRISPR screening, ALK, Resistance, NF1, NRAS, Trametinib, Lorlatinib, Ceritinib, Collateral sensitivity

Background

The development of molecular targeted therapies has significantly improved survival in a subset of cancer patients [1]. However, initial good responses to targeted therapies are frequently followed by resistance development [2, 3], preventing curative treatment in most cases using single-agent treatments. Once resistance develops, treatment options are often lacking. Intriguingly, some alterations conferring resistance to targeted therapies can also lead to new vulnerabilities, specifically in resistant cells, a concept termed collateral sensitivity [4].

Anaplastic lymphoma kinase (ALK) is a receptor tyrosine kinase frequently altered in cancers, either through chromosomal translocations leading to fusion of the ALK kinase domain with the amino-terminus of other proteins, or through activating point mutations or focal gene amplifications. *ALK* fusion genes drive tumorigenesis across a variety of different malignancies including anaplastic large cell lymphoma (ALCL) [5], non-small-cell lung cancer (NSCLC) [6] and inflammatory myofibroblastic tumor (IMT) [7]. Treatment with small molecule inhibitors for ALK, like ceritinib or lorlatinib, can be effective in a subset of patients, and ALK inhibitors have since entered routine and first-line therapy for many cancer entities [8, 9]. As observed with other targeted therapies, resistance to ALK inhibitors frequently occurs in *ALK*-driven cancer. While mechanisms leading to ALK inhibitor resistance in cancers with *ALK* fusion genes have been extensively studied [10], the mechanisms in tumors containing activating ALK mutations or *ALK* amplifications are largely unknown.

Neuroblastoma, a childhood tumor originating from the sympathetic nervous system [11], is a prototypical example of a cancer with recurrent *ALK* mutations. At diagnosis, up to 15% of neuroblastomas harbor activating point mutations or amplifications of *ALK*, and *ALK* mutations are further enriched upon disease relapse [12–20]. Mutated *ALK* is a driving oncogene in neuroblastoma, and neuroblastoma cells have a persistent and strong dependency on mutated ALK [21]. Activating mutations most often occur in the kinase domain, leading to increased ALK downstream signaling via the PI3K/AKT, RAS/MAPK and JAK/STAT pathways, promoting neuroblastoma cell survival and proliferation

[14–19, 22–24]. Despite multimodal therapy including chemotherapy, surgery, radiation therapy and immunotherapy [25], high-risk neuroblastoma, often harboring *ALK* alterations [26], remains very difficult to treat [20, 27–29].

The initial optimism that ALK inhibitors could improve neuroblastoma outcome has been tempered by our recent understanding that the second most prevalent *ALK* mutation in sporadic neuroblastoma, ALK F1174L is intrinsically resistant to the first-generation ALK inhibitor, crizotinib [30, 31]. In contrast, phase I trials with the second-generation ALK inhibitor, ceritinib, showed clinically relevant responses in a fraction of patients with refractory or relapsed neuroblastoma, but the response duration was short, indicating early resistance development [32]. The third-generation ALK inhibitor, lorlatinib, is currently being evaluated to treat relapsed neuroblastoma in a phase I/II trial [33], and may soon be introduced into first-line therapy trials. Thus, understanding ALK inhibitor resistance mechanisms in neuroblastoma is of utmost clinical importance.

Only few mechanisms of ALK inhibitor resistance have been detected in preclinical models of neuroblastoma so far, most of which were adaptive epigenetic or gene expression changes that have not yet been observed in patients developing resistance and may not be therapeutically actionable [34–36]. Here, we aimed to identify clinically relevant genetic mechanisms of ALK resistance and collateral sensitivities resulting from such alterations. We recurrently detected *NF1* loss-of-function mutations as well as activating mutations in *RAS* and its analogues in clinical samples from ALK inhibitor-resistant neuroblastomas and confirmed the causal contribution of these mutations to ALK inhibitor resistance in preclinical models. Moreover, we identified hypersensitivity to MEK inhibition as a novel collateral sensitivity specific to *NF1* loss, which may represent a clinically actionable therapeutic strategy for ALK-inhibitor resistant neuroblastoma.

Methods

Cell lines

The human neuroblastoma cell lines Kelly (#ACC 355, female), SH-SY5Y (#ACC 209, female) and LAN-5

(#ACC 673, male) were obtained from DSMZ. NBLW-R were provided by the university of Chicago on behalf of Susan Cohn. All cell lines were cultured in a RPMI 1640-based medium (Life Technologies, #21875035). For NBLW-R this medium was supplemented with 10% fetal calf serum (FCS Superior, Sigma, #S0615) and for SH-SY5Y and Kelly with an additional 1% penicillin/streptomycin (Gibco, #15140122). For LAN-5 the medium was supplemented with 20% FCS, 1% penicillin/streptomycin, 1x non-essential amino acids (Roth, #9185.1) and 1x GlutaMAX (Gibco, #35050061). *NFI* knockout single cell clones were cultured under the same conditions as the respective parental cell line. All cell lines were incubated at 37°C and 5% CO₂. Lorlatinib-resistant NBLW-R.L2 and ceritinib-resistant NBLW-R.C1 were generated by exposure to increasing concentrations (20nM to 10µM) of lorlatinib or ceritinib for a time of 3 months. Both cell lines were cultured as the parental line and 20nM lorlatinib or 20nM ceritinib added respectively. SH-SY5Y TR were cultured in RPMI 1640, 10% FCS, 1% penicillin/streptomycin and 5µg/ml Blastidicin (Invitrogen, #R210-01). For SH-SY5Y TR NRAS^{Q61K} cells 0.4mg/ml G418 (Genaxxon, #M3118.0050) was added as well. Cell line identities of SH-SY5Y and LAN-5 cell lines and their respective *NFI* knockout single cell clones as well as for Kelly and SH-SY5Y TR were confirmed by STR profiling at the DSMZ. Cell lines were regularly tested for Mycoplasma using the Plasmotest kit (InvivoGen, #rep-pt1). HEK293FT (female) were purchased from Thermo Fisher (#R7007) and cultivated in DMEM (Gibco, #61965026) according to manufacturer instructions. For details on cell line model generation please see Additional file 6 supplementary methods.

Chemicals

Lorlatinib, ceritinib, trametinib, rapamycin and pictilisib were purchased from Axon Medchem (#Axon2600, #Axon224, #Axon1761, #Axon2069, #Axon1377). Lorlatinib was given from Pfizer for in vivo studies with the NBLW-R. LY3009120 was bought from Selleck Chemicals (#S7842).

CRISPR-Cas9 knockout screen

For the CRISPR-Cas9-based negative selection screens performed in the neuroblastoma cell line SH-SY5Y, the human CRISPR knockout library Brunello was used as a one-vector system (Addgene, #73179) [37]. The pooled plasmid library targeting 19,114 genes with 76,441 sgRNAs (average of 4 sgRNAs per gene) was amplified as described elsewhere [37]. For details on library amplification and lentiviral production of the pooled plasmid library please also see Additional file 6 supplementary methods. To achieve the integration of one sgRNA per

cell an MOI of 0.3 was used. To maintain a 1000x representation of each sgRNA at the timepoint of transduction $7 \times 36.4 \times 10^6$ SH-SY5Y cells were transduced per T300 flasks. 24 hours post transduction medium was changed. 48 hours post transduction puromycin selection medium (0.8µg/ml puromycin, Thermo Fisher, #A1113803) was added to the cells and selection stopped after 6 days. Positively selected cells were expanded for 14 days to perform the screen with a ~1000x coverage. At d₀ one sample was harvest as baseline sample (t₀) and the other samples treated in two technical replicates with DMSO, ceritinib (0.3µM, Axon Medchem, #2224) or lorlatinib (0.1µM, Axon Medchem, #2600) for a total of 13 days. Medium was changed every third day. Cells were harvested on day 13 with a coverage of at least ~500x per condition. Genomic DNA (gDNA) was isolated using the ZymoResearch Quick-gDNA MidiPrep (ZymoResearch, #D4075). PCR amplification and high-throughput sequencing for sgRNA quantification are described below. Sequencing data was analyzed using MAGeCK-VISPR [38].

Quantification of sgRNAs

To confirm the maintenance of the library representation after amplification of the pDNA pool, the library was amplified by PCR (cycling conditions: 1 × 1 min at 95°C, 28 cycles of 30 s at 95°C, 30 s at 53°C, 30 s at 72°C and 1 × 10 min 72°C) using P5 primer mix and P7 A01 (Additional file 5 Table S5) as described elsewhere [39]. After gel extraction using the NucleoSpin Gel and PCR-Clean Up kit (Macherey-Nagel, #740609.50) the sample was also bead purified using the AMPure XP PCR purification protocol (Beckman coulter, #63880). After quality control experiments the sample was submitted for sequencing using the paired-end 150 MiniSeq Mid Output kit (Illumina, #FC-420-1004) with 10% PhiX. After confirmation of library representation, the pDNA pool was used for virus production. Genomic DNA of samples of the CRISPR/Cas9-based negative selection screen with ALK inhibitors was isolated as described above and used for PCR to quantify sgRNAs. A total of 26µg genomic DNA per condition were used to perform 12 PCR reactions per sample to maintain a good representation (per reaction: 2.2µg gDNA, 1µM of primer mix P5, 1µM of specific P7 primer per condition, 50µl of Ultra II Q5 Master Mix Polymerase (NEB, #M0544L) and water for a total reaction volume of 100µl). PCR cycling conditions: 1 × 1 min at 95°C, 28 cycles of 30 s at 95°C, 30 s at 53°C, 30 s at 72°C and 1 × 10 min 72°C. PCR products were gel purified using the NucleoSpin Gel and PCR-Clean Up kit (Macherey-Nagel, #740609.50). Samples were sequenced as a pooled library using a NextSeq 550 sequencer, the paired-end 150 High Output kit (Illumina, #20024907)

and 10% PhiX. The sequences of the primers used for PCR analyses are described in Additional file 5 Table S5.

RT-qPCR

RNA was isolated with TRIzol™ Reagent (Invitrogen, #15596026) according to manufacturer guidelines. To determine mRNA expression 1 µg or 500 ng RNA were incubated for 10 min at 65 °C with oligo (dT)₁₈ primer and transcribed into cDNA using the transcriptor first strand cDNA synthesis kit (Roche, #04379012001) (55 °C for 30 min, 50 °C for 1 hour, 85 °C for 5 min). For qPCR performance on a QuantStudio™3 Real-Time PCR System (Applied Biosystems™, #A28567) a 1:4 dilution of cDNA was mixed with 5 µl FastStart Essential DNA Green Master (Roche, #06402712001) and primers (Additional file 5 Table S5). Quantitative PCR cycling conditions: 50 °C for 2 min, 95 °C for 10 min, [95 °C for 15 s, 60 °C for 1 min, 95 °C for 15 s] (40 cycles), 60 °C for 1 min and 95 °C for 15 s. For each sample technical duplicates were prepared and a total of three biological replicates.

Drug treatments and cell viability measurement

For inhibitor treatments the cell lines Kelly, LAN-5 (5000 cells/well), SH-SY5Y (3000 cells/well), NBLW-R, NBLW-R.LR, NBLW-R.CR (each 10,000 cells/well) as well as SH-SY5Y TR and respective model systems were seeded in white 96-well plates 24 hours before the inhibitor treatment. Inhibitors dissolved in DMSO were applied using a Tecan D300e digital dispenser and each concentration was added with 3 technical replicates. Cell viability assessed after 72 hours (or 10 days for NBLW-R, and 5 days for NBLW-R.LR or NBLW-R.CR) using the ATP quantification assay CellTiter-Glo® (Promega, #G7571) according to manufacturer protocol. To determine cell numbers during and after 72 hours of inhibitor treatment experiments with the live-cell imaging system Incucyte® S3 (Sartorius) were performed. Therefore, LAN-5, SH-SY5Y as well as SH-SY5Y TR and respective model systems were seeded according to their specific growth rate in clear 96-well plates 24 hours before the inhibitor treatment (LAN-5 15,000 cells/well, LAN-5 *NF1* KO#1 17,000 cells/well, LAN-5 *NF1* KO#2 17,000 cells/well, SH-SY5Y 15,000 cells/well, SH-SY5Y *NF1* KO#1 19,000 cells/well, SH-SY5Y *NF1* KO#2 8000 cells/well, SH-SY5Y TR EV and respective NRAS^{Q61K} clones 8000 cells/well). For each well 4 images using a 10x objective were taken and analyzed using the cell-by-cell module. For each experiment at least 3 biological replicates were conducted. Evaluation of data and generation of concentration-response curves was performed using GraphPad Prism 9.0 and the four-parameter logistics model.

Perturbation experiments and computational modelling

Respective cell lines were seeded, and serum starved for 24 hours. Cells were exposed to different inhibitors, ceritinib (SH-SY5Y: 600 nM, LAN-5: 337 nM), lorlatinib (LAN-5: 478 nM), trametinib (SH-SY5Y: 49 nM, LAN-5: 31 nM), pictilisib (SH-SY5Y: 1 µM, LAN-5: 31 nM), rapamycin (SH-SY5Y and LAN-5: 100 nM) or DMSO for 90 minutes. Subsequently cells were stimulated with 25 ng/ml EGF (R&D systems, #AFL236–200), 100 ng/ml IGF-1 (R&D systems, #291-G1–200) or PBS for 30 minutes. Cells were harvested using cell scrapers on ice and lysed using the Bio-Plex Pro Cell signaling reagent kit (Bio-Rad, #171304006M). Subsequently lysates were incubated with antibody-coated magnetic beads as described elsewhere [40]. Beads were specific for P-AKT (S473), P-ERK1/2 (Thr202/Tyr204/Thr185/Tyr187), P-MEK1 (S217/S221) and P-S6K (Thr389). Samples were analyzed using the Bio-Plex MAGPIX multiplex reader (Bio-Rad). Result files were further analyzed using the R package LXB (<https://cran.r-project.org/web/packages/lxb/index.html>) and a custom script to generate MIDAS-formatted files (following *DataRail* [41]). Subsequently perturbation data was used for computational modeling using the R package STASNet [42] (<https://github.com/molsysbio/STASNet>).

Western blot for treatment

Samples for western blot analysis of ALK downstream signaling during inhibitor treatment were prepared the following: cells were seeded, and serum starved for 24 hours. SH-SY5Y cells were treated with 49 nM trametinib (LAN-5: 31 nM), 600 nM ceritinib (LAN-5: 337 nM) or DMSO for a total 1 hour which included 30 minutes of stimulation with 25 ng/ml EGF (R&D systems, #AFL236–200) EGF or PBS (Carrier). NBLW-R cells were seeded, and serum starved for 24 hours, then treated with 100 nM of either ceritinib, lorlatinib, trametinib or DMSO for 1 hour which included 30 minutes of stimulation with 25 ng/ml EGF or PBS. Cells were harvested on ice using a cell scraper in cell lysis buffer (15 mM HEPES, 150 mM NaCl, 10 mM EDTA, 2% Triton X-100, pH 7.5, 1xPhosSTOP, 1xComplete Mini EDTA free protease inhibitor, 10 µg/ml Leupeptin, 10 µg/ml Aprotinin, 200 µM PMSE, 25 mM NaF) [43]. Determination of protein concentration, SDS-PAGE as well as semi-dry blots were performed as described in Additional file 6 supplementary methods.

Illustration tool

Graphical schemes were created with BioRender.

Quantification and statistical analysis

GraphPad Prism 9.0 was used to generate concentration response curves and to perform statistical analyses. Statistical tests used are specified in the Figure legends. Error bars represent mean \pm SD unless otherwise indicated in the figure legends.

For details on plasmid library amplification, lentivirus production and transduction, cell line model generation, protein lysate preparation and western blot, in vivo studies, whole-exome sequencing of cell lines, high-throughput drug screen, droplet digital PCR of NBLW-R cells, panel sequencing of tumor samples and panel sequencing of cfDNA samples, please see Additional file 6 supplementary methods.

Results

A genome-wide CRISPR knockout screen identifies *NF1* as a mediator of ALK inhibitor sensitivity

To identify genes mediating an ALK inhibitor-resistant phenotype in neuroblastoma cells, we performed a genome-wide CRISPR-Cas9-based knockout screen in neuroblastoma cells incubated in the presence or absence of ALK inhibitors. Prior to screening, we investigated ALK inhibitor responses of ALK-mutated neuroblastoma cell lines harboring *MYCN* amplifications (Kelly^{ALKF1174L}, LAN-5^{ALKR1275Q}) or non-amplified *MYCN* (SH-SY5Y^{ALKF1174L}) (Additional file 1 Fig. S1) to select a cell line and establish suitable ALKi concentrations for screening. The screen was performed in SH-SY5Y cells transduced with the genome-wide lentiviral single guide RNA (sgRNA) Brunello library [39] and with lorlatinib or ceritinib concentrations leading to 70–80% reduction of growth for 13 days (Fig. 1a). These samples were compared to SH-SY5Y cells incubated with DMSO as a control. Abundance of sgRNA sequences were quantified by next-generation sequencing before (t_0) and 13 days after treatment and read count matrices were used for MAGeCK-VISPR analysis [38]. Based on MAGeCK-VISPR 'β' scores, we identified 109 genes with significantly enriched gene-targeting sgRNAs ($P \leq 0.01$) in cells treated with either ALK inhibitor (Fig. 1b). Technical screen replicates for each treatment showed a high correlation ($r \geq 0.98$) of normalized counts per sgRNA (Additional file 1 Fig. S2a and S2b). According to the published literature, some of these genes were members of ALK downstream signaling pathways, such as the JAK/STAT pathway and Src signaling (Additional file 3 Table S3). Most interestingly, all sgRNAs targeting *NF1*, a Ras-GTPase activating protein (Ras-GAP) and negative regulator of Ras signaling [44], were among the most significantly enriched in cells treated with either ALK inhibitor (Fig. 1b and c), suggesting *NF1* to be crucial for ALK inhibitor response. Thus, loss of proteins modulating

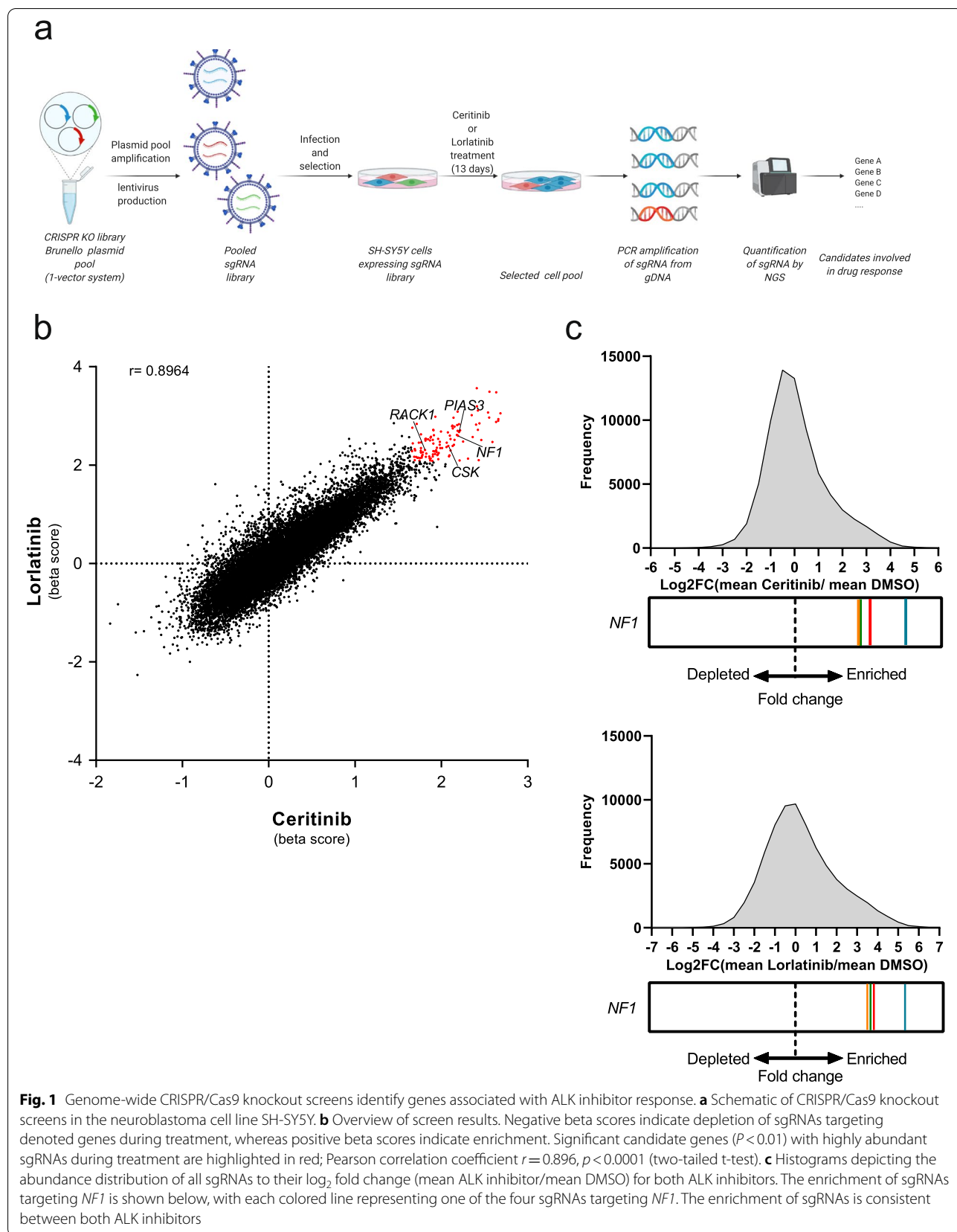
ALK downstream signaling, and *NF1* particularly, may lead to ALK inhibitor resistance.

NF1 knockout results in ALK inhibitor resistance

To formally demonstrate that loss of *NF1* can cause ALK inhibitor resistance in neuroblastoma cell lines, we generated several neuroblastoma cell line models harboring *NF1* knockouts. We used the neuroblastoma cell lines SH-SY5Y (*ALK*^{F1174L}) and LAN-5 (*ALK*^{R1275Q}, *MYCN*-amplified), to represent ALK-mutated neuroblastoma within a genomic background either with or without *MYCN* amplification. The absence of mutations in ALK downstream signaling pathways was verified in these cell lines by targeted and exome sequencing. *NF1* knockouts were introduced using CRISPR-Cas9 targeting exon 1 or 30. After generating and validating isogenic cell lines for *NF1* knockout (Fig. 2a), we observed increased RAS/MAPK signaling as seen by an increased phosphorylation of ERK1/2 in *NF1* knockout clones (Fig. 2b), in line with *NF1* function in this pathway [45]. Sensitivity towards ALK inhibition was significantly reduced in cells lacking *NF1*, as assessed by treatment of the cells with lorlatinib or ceritinib for 72 hours and determination of cell viability (Fig. 2c, d, Additional file 1 Fig. S7a and S7b). These data demonstrate that loss of *NF1* is sufficient to cause ALK inhibitor resistance in ALK-mutated neuroblastoma cell lines.

NRAS mutations spontaneously arise during resistance development to ALK inhibitors

In order to explore de novo mutations occurring during development of ALK inhibitor resistance, we cultivated NBLW-R neuroblastoma cells (*ALK*^{F1174L}, *MYCN*-amplified) with increasing concentrations of lorlatinib or ceritinib for a period of 3 months (Fig. 3a) to generate resistant cell lines. Targeted sequencing was performed at the end of treatment, detecting recurrent *NRAS* mutations, c.C181>A or c.A182>G, both known to result in constitutively active RAS (*NRAS*^{Q61K} or *NRAS*^{Q61R} respectively) and increased signaling downstream of MAPK [46]. In addition, this was validated using droplet digital PCR (ddPCR) (Additional file 1 Fig. S3a). Each resistant cell line also demonstrated cross-resistance to alternative ALK inhibitors in comparison to the parental line, suggesting structure-independent resistance (Fig. 3b, c and Additional file 1 Fig. S3b). Activation of *NRAS* in these models was confirmed by western blotting for phosphorylated ERK1/2 following treatment with ALK inhibitors in resistant cells compared to the parental cell lines as controls. ERK1/2 remained phosphorylated in the resistant cell models even after treatment with higher concentrations of ALK inhibitors (Fig. 3d). Maintenance of ALK dephosphorylation after treatment



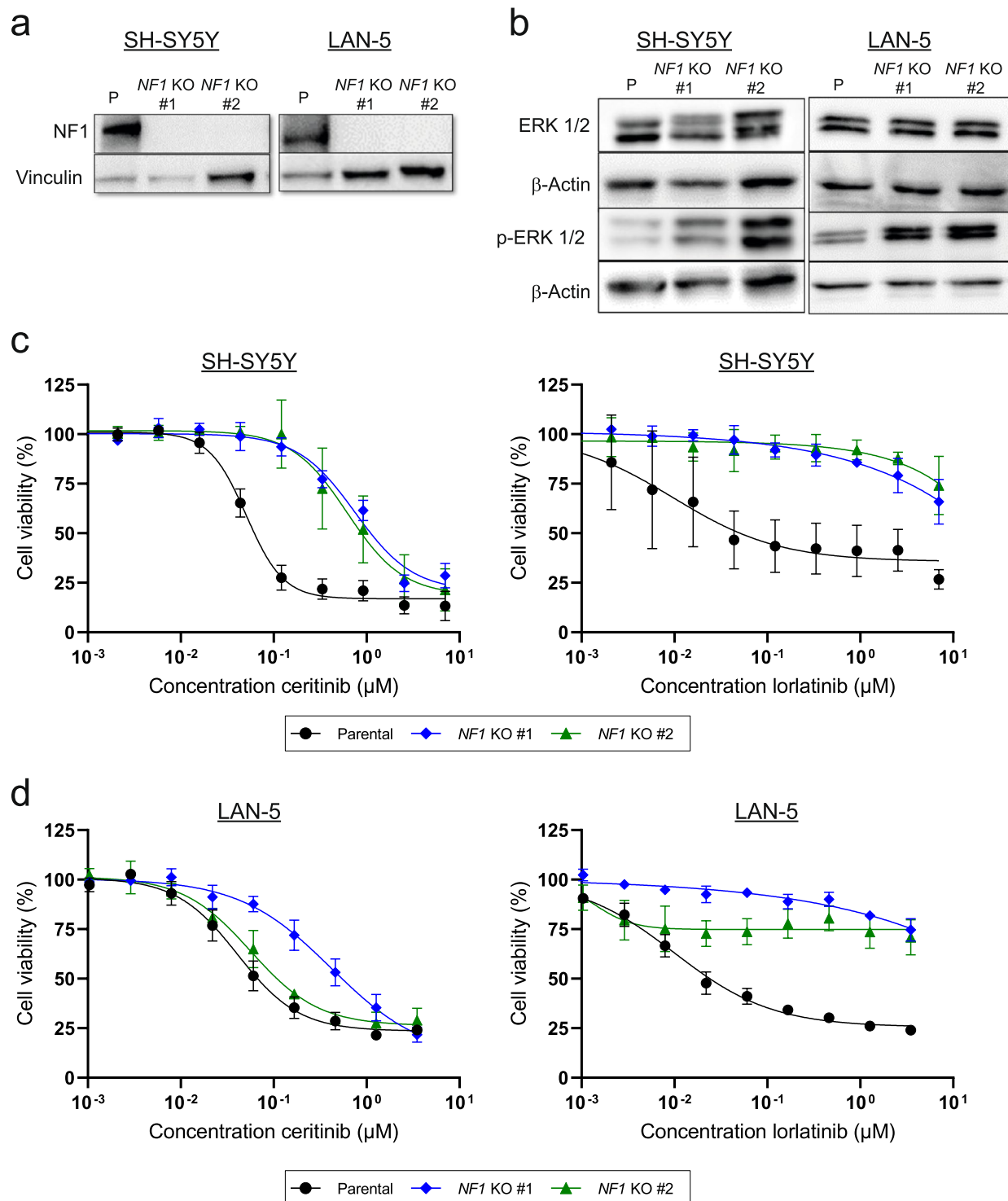
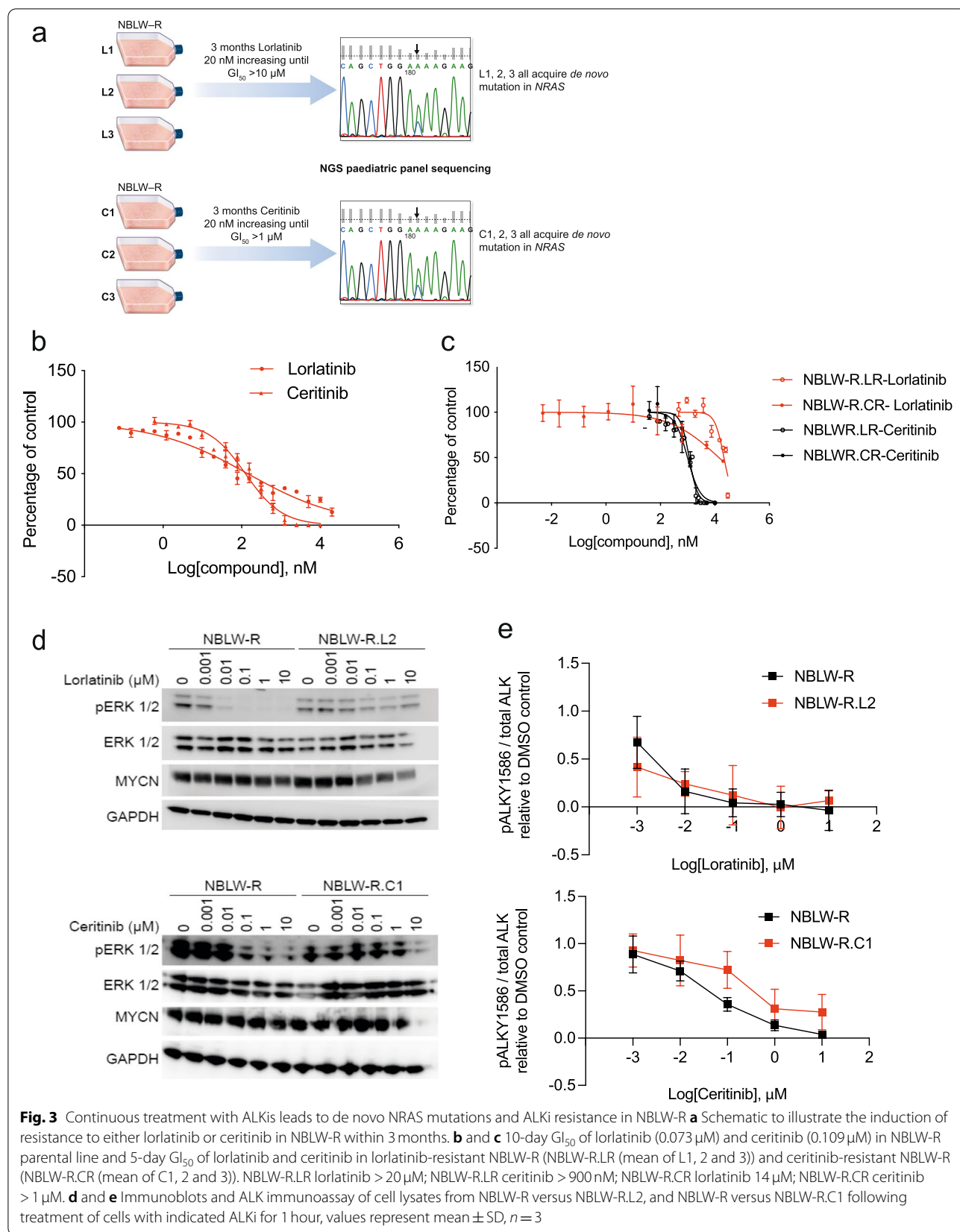


Fig. 2 *NF1* knockout leads to ALK inhibitor resistance in neuroblastoma cell lines. **a** Knockout of *NF1* in different ALK-mutated neuroblastoma cell lines using CRISPR-Cas9 leads to an absence of *NF1* protein. **b** Western blot analysis of total and phosphorylated ERK 1/2 indicates increased RAS/MAPK signaling in *NF1* knockout single-cell clones. **c** and **d** Cell viability of *NF1* knockout clones was assessed during ALK inhibitor treatment with ceritinib or lorlatinib and indicated decreased cell sensitivity; values represent mean ± SD, *n* = 3



was confirmed by immunoassay (Fig. 3e). MRI scans and growth analysis in an orthotopic kidney capsule murine model revealed that both lorlatinib- and ceritinib-resistant cells formed tumors more quickly than parental NBLW-R cells (Additional file 1 Fig. S3c and S3d). In line with our in vitro results, lorlatinib or ceritinib treatment of mice engrafted with ceritinib-resistant NBLW-R lines demonstrated significantly reduced efficacy of lorlatinib compared with mice engrafted with parental NBLW-R cells (Additional file 1 Figure S3e). These data suggest that both NF1 loss and acquisition of activating NRAS mutations, either of which can activate MAPK signaling, can induce ALK inhibitor resistance.

Expression of mutant NRAS leads to ALK inhibitor resistance

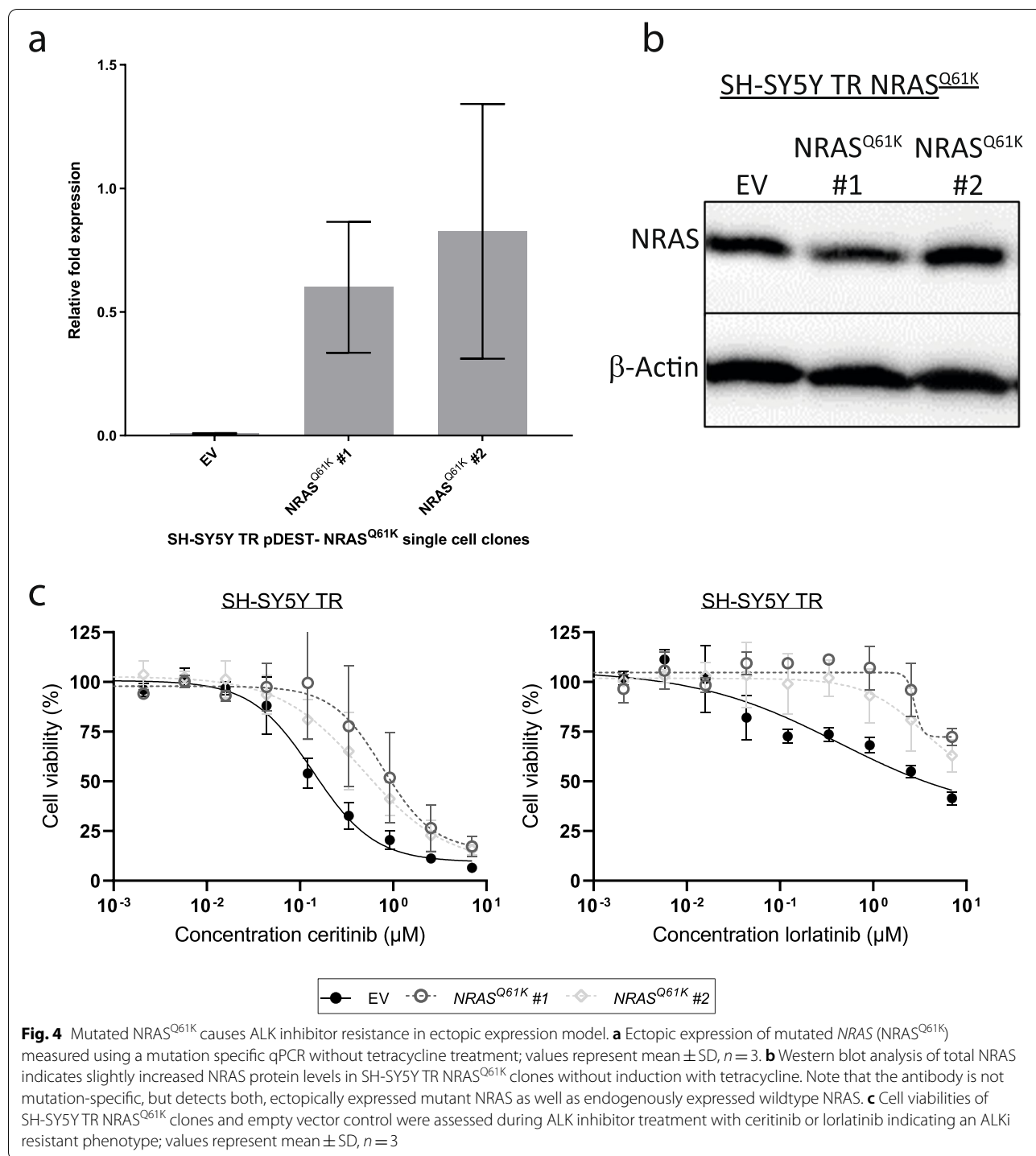
To investigate whether the NRAS^{Q61K} mutant, which arose in cells spontaneously developing ALK inhibitor resistance, is sufficient to induce ALK inhibitor resistance, we generated SH-SY5Y cells inducibly expressing NRAS^{Q61K} (tetracycline-dependent). We analyzed NRAS expression in two independent clonal cultures as well as an empty vector control cell clone, using western blotting and RT-qPCR. RT-qPCR revealed strong induction of NRAS^{Q61K} by tetracycline treatment (Additional file 1 Fig. S4). In line with the results of RT-qPCR, western blot experiments revealed strong induction of NRAS by tetracycline treatment, with western blot being unable to discriminate between wildtype NRAS and mutated NRAS^{Q61K} (data not shown). However, significant expression of NRAS^{Q61K} was detected by mutation-specific RT-qPCR also in the absence of tetracycline compared to the empty vector control (Fig. 4a). This suggested a significant leakiness of our expression system, rendering comparisons of clones in the absence and presence of tetracycline less effective. Instead, we compared cells expressing NRAS^{Q61K} to the empty vector control cells in the absence of tetracycline. While NRAS^{Q61K} was clearly expressed in the NRAS^{Q61K}-transfected clones in the absence of tetracycline (as detected by mutation specific RT-qPCR) and was completely absent in the empty vector control cells, western blot analysis revealed that overall NRAS protein levels did not relevantly exceed baseline levels in the NRAS^{Q61K}-transfected clones as compared to empty vector control cells (Fig. 4b), which allowed us to specifically analyze the effect of the presence of the Q61K mutation rather than the effect of excessive NRAS expression. Cells expressing NRAS^{Q61K} were significantly more resistant to either lorlatinib or ceritinib compared to isogenic control cells harboring the empty vector (Fig. 4c). This demonstrates that NRAS^{Q61K} mutation is sufficient to induce an ALK inhibitor resistant phenotype in neuroblastoma cell lines.

NF1 loss-of-function mutations and activating RAS mutations occur in ALK inhibitor-resistant relapsed human neuroblastomas

In order to investigate the clinical relevance of our observations that both NF1 loss and NRAS activation were sufficient to induce ALK inhibitor resistance in neuroblastoma models, we genomically profiled tumor and liquid biopsy samples (whole-exome sequencing or a hybrid-capture targeted next-generation sequencing assay) from four patients with neuroblastomas harboring activating ALK mutations before ALK inhibitor treatment and during tumor progression under treatment (Fig. 5a, also see Table S1). In line with our observations in preclinical models, known loss-of-function NF1 mutations (NF1^{R1276*}, NF1^{A320fs} and NF1^{F1593S}) occurred de novo in two patients after treatment with ceritinib (Fig. 5b). In samples from two patients treated with lorlatinib we detected de novo NRAS (Fig. 5c) or HRAS mutations (NRAS^{Q61K} and HRAS^{Q61K}), associated with constitutively activated RAS protein of the respective isoform [47, 48]. These observations further affirm the clinical relevance of NF1 and RAS in ALK inhibitor resistance in neuroblastoma.

Loss of NF1 causes increased RAS-MAPK signaling and diminished negative ERK-RAF feedback

To understand how loss of NF1 alters ALK signaling pathways and to potentially identify collateral sensitivities pointing toward new treatment options for patients with disease resistant to ALK inhibitors, we performed perturbation experiments and subsequent computational modeling of signaling networks using steady-state analysis of signaling networks (STASNet) [42]. NF1 knockout cell models and their parental controls were exposed to inhibitors targeting ALK, MEK, PI3K or mTOR and subsequently stimulated with the growth factors, EGF or IGF1. Relative phosphorylation of signaling components downstream of ALK was measured using a multiplexed bead-based ELISA assay (Fig. 6a). As expected, NF1 loss was associated with increased RAS-MAPK signaling (see also Fig. 2b), in line with the role of NF1 as a negative regulator of RAS/MAPK signaling [45]. The perturbation-response data (Fig. S5) together with a prior knowledge network of the signaling topology served as input for the STASNet signaling network modeling pipeline (Fig. 6b). The output of the modelling procedure are quantified signaling interactions and differences due to the NF1 knockout. More precisely, STASNet adjusts model parameters representing the strength of signaling interactions in the signaling network and inhibitor efficacy such that the model simulations fitted the data optimally. We constrained the model parameters of isogenic cell line triplets such that they were identical between



the isogenic cell lines triplets and allowed divergence of parameters between these cell lines only if it was necessary to fit the data, as quantified by a likelihood ratio test. This procedure reflected that molecular changes between isogenic cell lines were minimal and that we expected that most molecule interactions remain quantitatively

similar. When we inspected the model parameters that diverged, we noticed a weakened negative feedback from ERK to RAF in all *NFI* knockout clones in comparison to the parental cell lines (Fig. 6c, red box and Additional file 1 Fig. S5). Such a negative feedback restricts MAPK signaling in parental cells, and consequently EGF

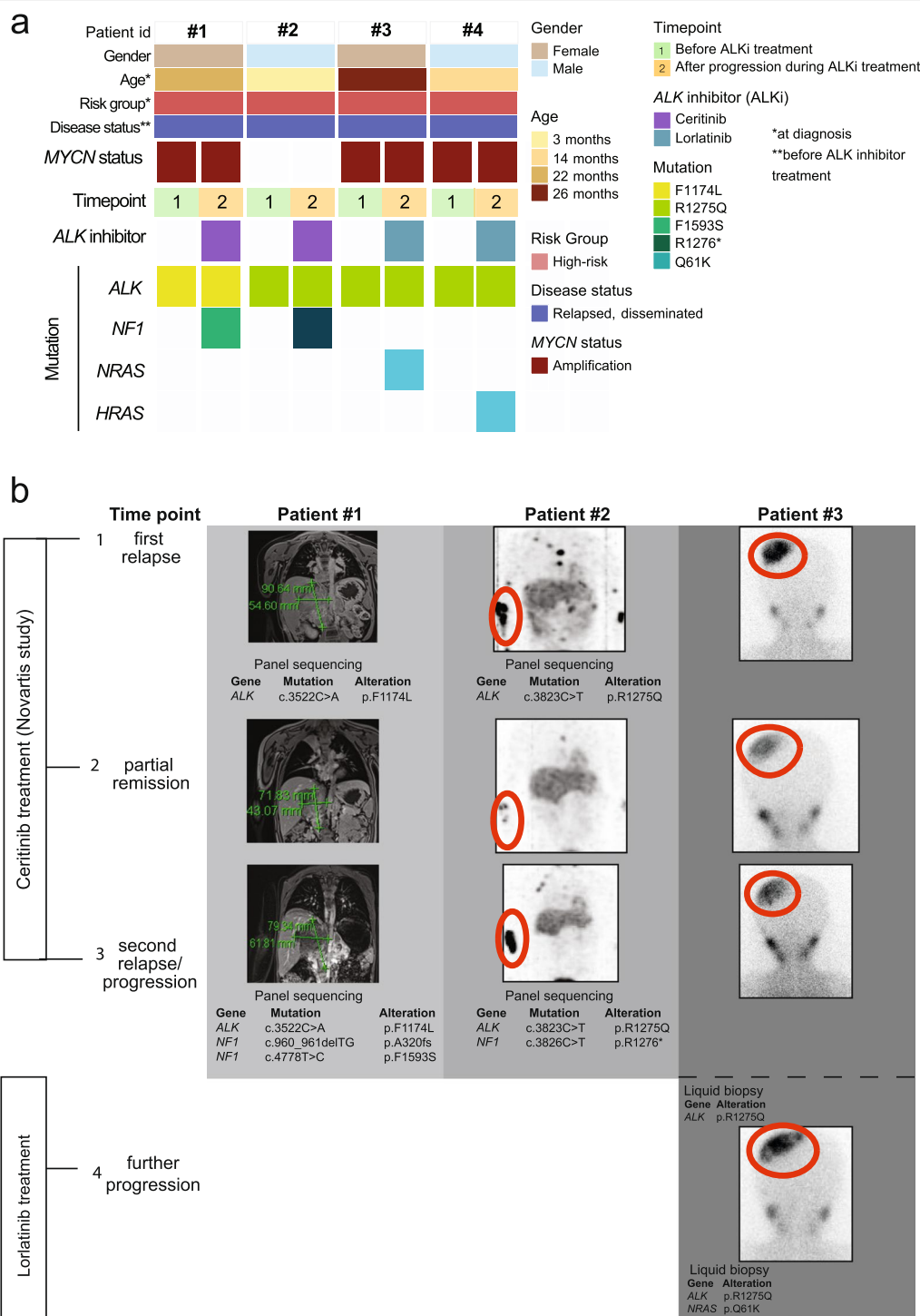
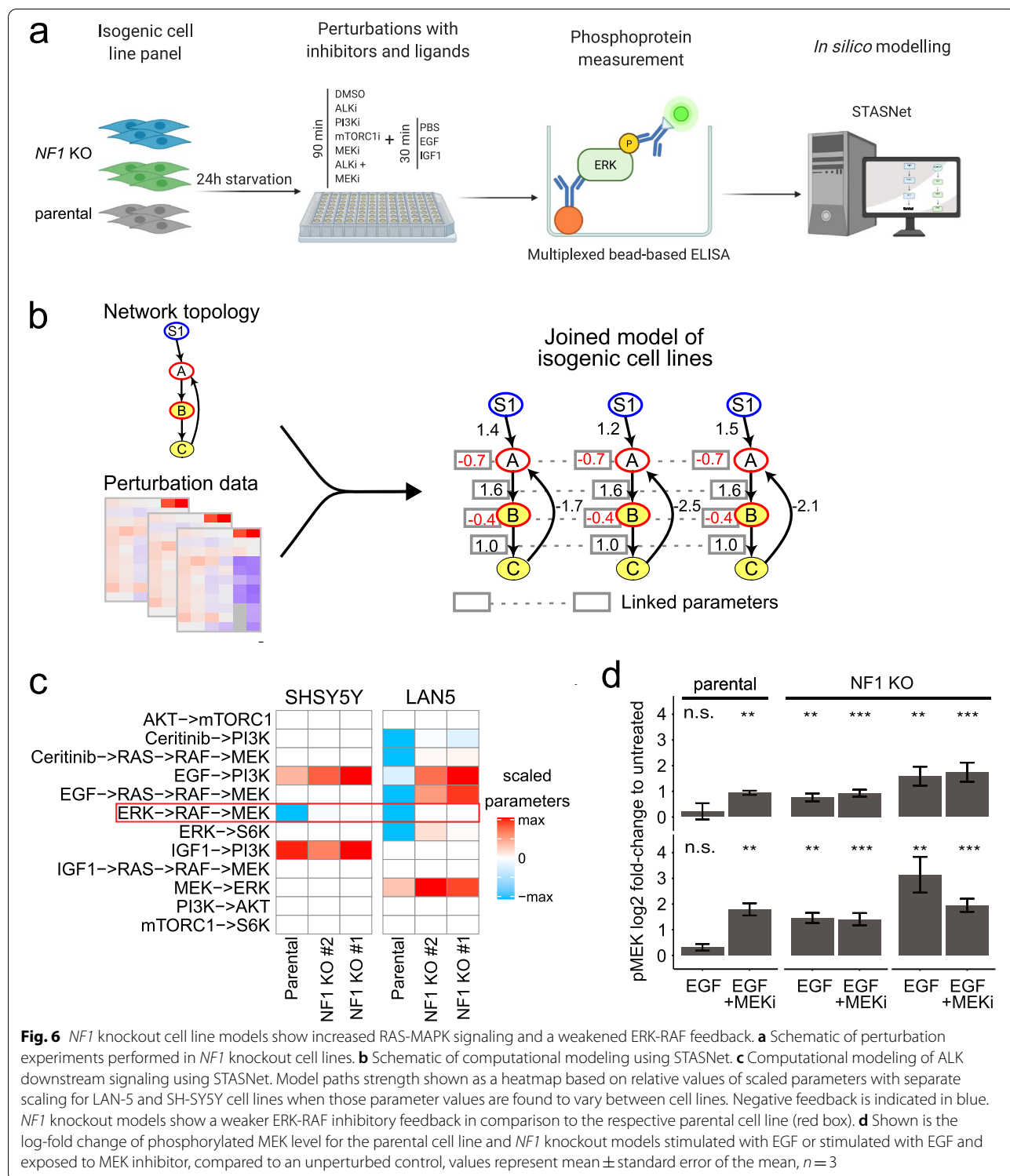


Fig. 5 Mutations in ALK downstream signaling cause ALK inhibitor resistance in ALK-mutated neuroblastoma. **a** Clinical covariates of the high-risk neuroblastoma cohort ($n = 4$) before and after development of ALK inhibitor resistance. **b** Magnetic resonance imaging (MRI) scans and Iodine-123 metaiodobenzylguanidine scintigraphy scans (MIBG) of patients whose tumors harbored ALK^{R1275Q} or ALK^{F1174L} mutations during treatment with ceritinib. After partial remission both, patient 1 and 2, relapsed under ceritinib treatment and de novo NF1 mutations were detected using targeted sequencing. Tumor lesions are highlighted by red circles. **c** MIBG- scans of patient whose tumor harbored ALK^{R1275Q} mutations during treatment with ceritinib and lorlatinib. After partial remission the patient relapsed under ALKi treatment and de novo NRAS mutations were detected using targeted sequencing. Tumor lesions are highlighted by red circles



activated MEK only when MEK inhibitors were present in parental cell lines, whereas EGF activated MAPK signaling efficiently in *NF1* knockout cells irrespective of MEK blockage (Fig. 6d). Strong negative feedback, as we detected in the parental neuroblastoma cell lines, is a known resistance mechanism against MEK inhibitors since it results in an accumulation of phosphorylated MEK leading to reactivation of downstream targets [49, 50]. Taken together, these results suggest that MAPK signaling upon *NF1* knockout in neuroblastoma cells harboring ALK mutations is associated with loss of negative ERK-RAF feedback, leading us to hypothesize that these cell lines may be particularly sensitive to MEK inhibitor treatment.

Deletion of NF1 in ALK-mutated neuroblastoma cells increases MEK inhibitor sensitivity

To test predictions derived from the computational modeling, we investigated MEK inhibitor sensitivity in *NF1* knockout models and ectopic NRAS^{Q61K} expression models by performing a small inhibitor screen for 4 inhibitors of signaling downstream of ALK. Indeed, *NF1* knockout clones were more sensitive than the parental cell line to MEK inhibition by trametinib as well as the pan-RAF inhibitor, LY3009120, (Fig. 7a and c). In contrast, sensitivity of *NF1* knockout clones towards the mTOR inhibitor, rapamycin, and the PI3K inhibitor, GDC0941, was unaltered or only slightly reduced from that in parental cell lines. *NF1* knockout cells, contrary to cells with ectopic NRAS^{Q61K}, were not differentially sensitive (compared with control cell lines harboring the empty vector) to any of the drugs screened (Fig. 7b, d and Additional file 1 S6a). A high-throughput screen of 197 drugs was also performed to compare drug sensitivities between the LAN-5 *NF1* KO #1 knockout clone and its parental line, which revealed a singular and specific hypersensitivity of the *NF1* knockout clone to different MEK inhibitors that was not present in the parental line (Additional file 1 Fig. S7a and S7c). Responses to ALK and MEK inhibitors were investigated in western blots from all cell lines, detecting low levels of MEK phosphorylation (Ser217/221)

and an absence of ERK phosphorylation in *NF1* knockout clones during trametinib treatment (Fig. 7e). These results were consistent with our computational modeling data, which indicated a weak or missing ERK-RAF feedback (Fig. 6d). Ectopic NRAS^{Q61K} expression (in comparison to *NF1* knockout clones) was associated with elevated MEK phosphorylation after EGF stimulation and ceritinib exposure. MEK phosphorylation in ectopic NRAS^{Q61K} expressing clones was comparable to levels detected for the empty vector control during trametinib treatment (Fig. 7f), indicating NRAS^{Q61K} expression did not alter ERK-RAF feedback. Responses of NBLW-R parental and resistant lines to trametinib further confirmed that de novo NRAS^{Q61K} acquisition seems to have no effect on the ERK to RAF feedback, as evidenced by their insensitivity to MEK inhibition and strong phosphorylated MEK levels after MEK inhibitor treatment (Fig. 7g). In conclusion, only *NF1* loss but not the expression of oncogenic NRAS^{Q61K} seems to trigger loss of feedback-mediated MEK reactivation and leads to increased sensitivity of neuroblastoma cell lines harboring ALK mutations to MEK inhibition. Our results suggest MEK inhibitor sensitivity is a new vulnerability and collateral sensitivity in a subset of ALK inhibitor-resistant neuroblastomas (Fig. 7h).

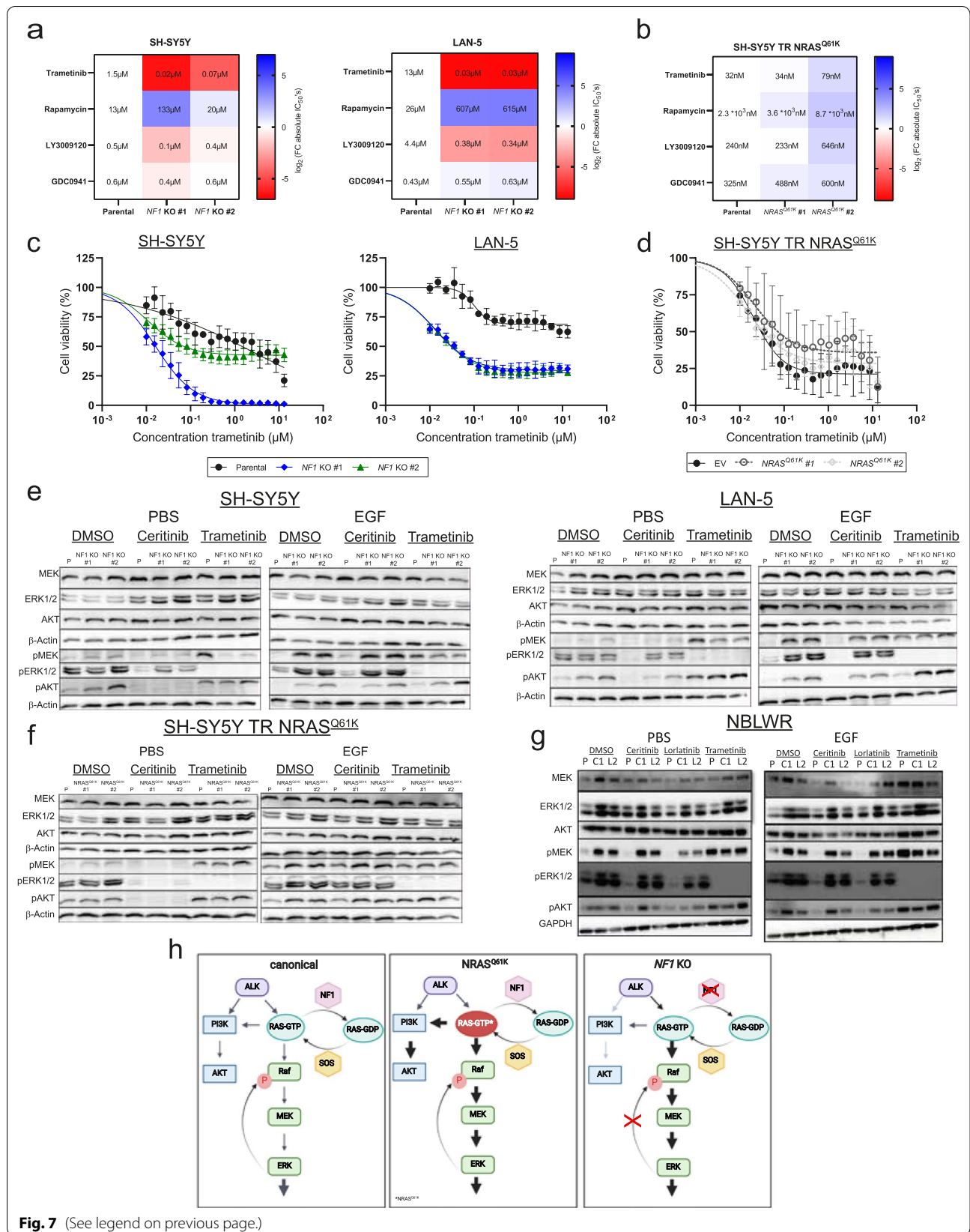
Discussion

Clinical responses to targeted inhibitors often do not translate into improved patient cure rates due to frequent development of therapy resistance [51, 52]. Improving cure rates, therefore, depends on our understanding of resistance mechanisms and the development of treatment strategies for therapy-resistant cancers. Here, we analyzed ALK inhibitor resistance in neuroblastoma, and demonstrated that loss of NF1 or mutation of NRAS^{Q61K} can lead to ALK inhibitor resistance. We identified MEK inhibitor sensitivity as a collateral sensitivity of ALK inhibitor resistance due to NF1 loss in ALK-mutated neuroblastoma cells.

To determine mechanisms of ALK inhibitor resistance, we first screened preclinical models and subsequently analyzed tumor samples or liquid biopsies obtained

(See figure on next page.)

Fig. 7 *NF1* knockout cell line models are sensitive to MEK and pan-RAF inhibitor treatment. **a** and **b** Drug screen of *NF1* knockout cell lines and ectopic NRAS^{Q61K} expression models. Cells were treated with trametinib (MEKi), rapamycin (mTORi), pictilisib (GDC0941, PI3Ki) or pan-RAF inhibitor LY3009120 for 72 hours and cell viability assessed using CellTiterGlo measurements. Colors indicate log₂(FC) of absolute IC₅₀ values to values of the parental or empty vector control cell lines. Red indicates a higher sensitivity in comparison to the parental cell line or empty vector control and blue a decreased sensitivity. Respective absolute IC₅₀ values are shown for each treatment. **c** and **d** Respective concentration-response curves of *NF1* knockout clones and ectopic NRAS^{Q61K} expression models for MEK inhibitor treatment with trametinib; values represent mean ± SD, *n* = 3. **e**, **f** and **g** Western blot analysis of 24-hour-serum-starved *NF1* knockout cell lines, ectopic NRAS^{Q61K} expression models and NBLW-R resistant models exposed to DMSO, ceritinib, lorlatinib or trametinib for 1 hour with subsequent stimulation for 30 minutes with EGF or PBS. **h** Schematic of canonical ALK downstream signaling in comparison to signaling in neuroblastoma cell lines with mutated NRAS^{Q61K} or a *NF1* knockout



from patients before and during ALK inhibitor treatment (before/after initial response and during disease progression). Preclinically, we performed two unbiased screens. A CRISPR/Cas9 knockout screen using two different ALK inhibitors, ceritinib and lorlatinib, determined genes associated with ALK inhibitor resistance. We identified genes encoding proteins regulating signaling downstream of ALK that were modulated by both ALK inhibitors, with the most interesting hit being *NF1*. In parallel, we generated resistant cell populations in an *ALK*-mutated neuroblastoma cell line through constant lorlatinib or ceritinib exposure. De novo *NRAS*^{Q61K} mutations arose but *NF1* loss was not observed in resistant populations created in the continuous exposure resistance model. This in vitro response is in line with our observation that *NF1* was lost and activating *RAS* mutations were acquired in samples from patients. The underlying determinants for these differences remain to be investigated, but our findings clearly suggest that the route to MAPK activation can differ.

Some recent publications also mainly reported mechanisms involving epigenetic rewiring or overexpression of receptor tyrosine kinases other than ALK, as mechanisms rendering neuroblastoma cells independent of ALK signaling [34–36], but their clinical relevance remained elusive to date. These mechanisms should be non-mutually exclusive with our observations, as they are driven by deregulated gene expression (e.g., *BORIS*, *AXL*, *PIMI1*) rather than resistance mutations. It will be important to investigate different contributions of individual genetic and epigenetic mechanisms in future studies. It may be reasonable to speculate that some genetic mechanisms observed in our study may be a cause of deregulated gene expression observed in other studies. In line with our results, an independent report suggested *NF1* alterations were potentially involved in ALK resistance [53] and a case report described a de novo *NRAS*^{Q61K} mutation upon development of ALK inhibitor resistance in a lorlatinib-treated neuroblastoma [54]. To our knowledge, our report is the first to extend these observations and provide mechanistic evidence for their causal relationship.

NF1 knockout and ectopic *NRAS*^{Q61K} expression confirmed that these alterations can confer ALK inhibitor resistance, independent of cell line context or ALK mutation type. Resistance was more pronounced against lorlatinib than ceritinib. We believe that the ALK specificity and affinity of these two inhibitors may cause these differences, with lorlatinib being more specific for mutant ALK, while ceritinib is known to be less specific with more off-target cytotoxic effects [55]. Such off-target toxicity of ceritinib may reduce the effect of *NF1* loss and *NRAS*^{Q61K} acquisition, compared to lorlatinib.

In line with our in vitro data, we detected de novo *NF1* and *NRAS* or *HRAS* mutations in neuroblastomas from patients treated with the ALK inhibitors, ceritinib or lorlatinib, at resistance development. Due to limited material from the respective tumors, the presence of relevant fractions of nonmalignant cells and technical limitations of the hybrid-capture panel sequencing analysis, it could not be unequivocally determined if a *NF1* wildtype allele was maintained or lost in the tumors of patients #1 and #2 after ALK inhibitor treatment. In addition, it remained elusive if the two *NF1* mutations detected in the tumor of patient #2 after ALK inhibitor treatment occurred in two separate clones or in one clone, and in the latter case if these mutations occurred in *cis* or in *trans*. It will be important to extend these findings to prospective studies, which will enable measurements of mutation incidence and a more detailed analysis of *NF1* alterations. Despite the small sample size, our observations in four independent patients provide strong evidence for the clinical significance of our preclinical findings, and represents, to our knowledge, the first analysis of this sort. Intriguingly, all neuroblastomas in patients treated with ceritinib acquired inactivating *NF1* alterations, whereas neuroblastomas in patients treated with lorlatinib acquired activating *RAS* mutations. We believe this unlikely to be due to mechanistic differences, but future prospective studies investigating such differences may be warranted.

While we report *NF1* and *RAS* mutations in the context of ALK resistance development in neuroblastoma, loss-of-function *NF1* mutations and activating *RAS* mutations, as well as other *RAS*-MAPK pathway-activating mutations have been observed in primary and relapsed neuroblastoma independent of ALK inhibitor treatment [20, 56, 57]. In contrast to our observations of *ALK* mutations co-occurring with *NF1* or activating *RAS* mutations, these mutations were mutually exclusive in neuroblastoma samples from patients not treated with ALK inhibitors. This suggests that whereas MAPK pathway activation in primary tumors can occur through mutually exclusive ways, additional activating alterations can rescue the repressed *RAS*-MAPK activity in the presence of ALK inhibitors. It is reasonable to speculate that this re-activation might also occur through other mutations that affect MAPK activity, which should be tested in future trials.

Our findings are in line with reports of *RAS*-MAPK signaling reactivation through the loss of *NF1* as a mechanism of resistance to other targeted therapies, including EGFR inhibition in lung cancer [58], BRAF inhibition in melanoma [59], BCR-ABL inhibition in chronic myeloid leukemia [60] and endocrine therapies in advanced breast cancer [61]. In contrast, activating *NRAS*^{Q61K} mutations

have mainly been reported as arising in the context of BRAF inhibitor resistance in melanoma [62–64].

A yet often underappreciated strategy builds on the hypothesis that resistance mutations induce new vulnerabilities, depicted collateral sensitivities, and uses these new vulnerabilities to design serial combination therapies, thereby taking advantage of the process of resistance development rather than trying to counteract it. We perturbed and computationally modeled signaling networks in our *NF1* knockout models to identify new vulnerabilities and potential new treatment options. We were able to show that *NF1* loss shifts signaling downstream from ALK from a broader distribution among the JAK/STAT, AKT/PI3K and RAS/MAPK pathways towards stronger signaling exclusively along the RAS-MAPK axis. Most importantly, modeling indicated that ERK-RAF feedback was weakened, which led us to predict MEK inhibitor sensitivity as a new collateral sensitivity that was confirmed in our small inhibitor screen in the *NF1* knockout cell line model. Most treatment-naïve neuroblastoma cells are only intermediately sensitive to MEK inhibitors [65], in line with the failure of MEK inhibitors in clinical trials to treat neuroblastoma [66]. Our *NF1* knockout models were, contrastingly, hypersensitive to MEK inhibitor treatment. Phosphorylated MEK and ERK 1/2 levels decreased during trametinib treatment in *NF1* knockout clones, whereas phosphorylated MEK levels increased in the respective parental lines, likely maintaining sufficient ERK activity for cell proliferation. The latter was also observed for our ectopic NRAS^{Q61K} expression model and ALK inhibitor-resistant NBLW-R cell populations. In this context, phosphorylated MEK levels during MEK inhibitor treatment correlate with the strength of the ERK to RAF feedback. Cell lines less responsive or resistant to MEK inhibitors have previously been shown to possess strong inhibitory ERK to RAF feedback that is abrogated upon MEK inhibition to result in even higher levels of phosphorylated MEK and reactivation of the pathway [49, 50]. Cell lines sensitive to MEK inhibitors, however, show only a weakened or absent negative ERK to RAF feedback, which we propose as the mechanistic reason for MEK inhibitor sensitivity in neuroblastoma cell lines lacking *NF1*. Accordingly, we recently demonstrated in work available on the bioRxiv preprint server that the strength of ERK to RAF feedback correlates with the level of MEK inhibitor sensitivity in neuroblastoma cell lines [65]. Surprisingly, even though *NF1* and NRAS^{Q61K} mutations both increase RAS/MAPK signaling, thereby conferring ALK inhibitor resistance, cells harboring these alterations respond differently to MEK inhibitor treatment. This appears to be due to the different strengths of ERK to RAF feedback. The mechanism by which *NF1* loss abrogates ERK to RAF feedback in

neuroblastoma cells harboring ALK mutations remains elusive, but this will not prevent a rapid translation of this collateral sensitivity into the clinic. However, further investigation of the mechanism in the future may help to develop new ways of overcoming the feedback reactivating of the RAS/MAPK pathway in *NF1* wild type neuroblastomas to render them sensitive to MEK inhibitors in general.

Conclusion

Our study identifies *NF1* loss and activating RAS mutations as bona fide clinically relevant causes of ALK inhibitor resistance in ALK-driven neuroblastoma and establishes reactivation of signaling downstream from the RAS-MAPK pathway as a mechanism of ALK inhibitor resistance. Extending the concept of collateral sensitivities, we identified MEK inhibitor hypersensitivity as a new vulnerability after *NF1* loss in ALK-mutated neuroblastoma cells. This presents a potential treatment option for patients with neuroblastomas that have lost *NF1* and are resistant to ALK inhibitors, with the potential to impact clinical practice and future clinical trial design.

Abbreviations

ALCL: Anaplastic large cell lymphoma; ALK: Anaplastic lymphoma kinase; ALKi: Anaplastic lymphoma kinase inhibitor; cfDNA: Circulating free DNA; CRISPR: Clustered regularly interspaced short palindromic repeats; ctDNA: Circulating tumor DNA; ddPCR: Droplet digital PCR; EGF: Epidermal growth factor; ELISA: Enzyme linked immunosorbent assay; ERK1/2: Extracellular signal-regulated kinase 1/2; IGF1: Insulin-like growth factor 1; IMT: Inflammatory myofibroblastic tumor; MAGeCK: Model-based Analysis of Genome-wide CRISPR/Cas9 Knockout; MAPK: Mitogen-activated protein kinase; MEK: MAP 2K, Mitogen-activated protein kinase kinase; MRI: Magnetic resonance imaging; *NF1*: Neurofibromin 1; NSCLC: Non-small-cell lung cancer; pDNA: Plasmid DNA; RT-qPCR: Real-time quantitative PCR; sgRNA: Single guide RNA; STASNet: Steady-state analysis of signaling networks.

Supplementary Information

The online version contains supplementary material available at <https://doi.org/10.1186/s12943-022-01583-z>.

Additional file 1: Figure S1: ALK inhibitor treatment of ALK-mutated neuroblastoma cell lines for optimized screening conditions (related to Figure 1). **Figure S2:** Quality control of CRISPR/Cas9 knockout screen (related to Figure 1). **Figure S3:** Lorlatinib- and Ceritinib-resistant NBLW-R neuroblastoma cells grow as aggressive tumors in the kidney capsule of nude mice (related to Figure 3). **Figure S4:** Tetracycline induced NRAS^{Q61K} expression (related to Figure 4). **Figure S5:** Computational modeling of ALK downstream signaling using STASNet (related to Figure 6). **Figure S6:** MEK inhibitor treatment of ectopic NRAS^{Q61K} expression models (related to Figure 7). **Figure S7:** High-throughput drug screening of LAN-5 and LAN-5 *NF1* KO#2 clone (related to Figure 7). **Table S1.** Full clinical data on neuroblastoma patients.

Additional file 2: Table S2. Normalized read counts. CRISPR-Cas9 knockout screen-Normalized read counts (related to Figure 1).

Additional file 3: Table S3. MAGeCK VISPR analysis. CRISPR-Cas9 knockout screen-MAGeCK VISPR analysis (related to Figure 1).

Additional file 4: Table S4. Gene beta scores cutoff at p0.01. CRISPR-Cas9 knockout screen- Gene beta scores cutoff at p0.01 (related to Figure 1).

Additional file 5: Table S5. Oligonucleotides used. Oligonucleotides used in this study (related to Figures 1, 2 and 4).

Additional file 6. Supplementary Materials and Methods.

Acknowledgements

We especially thank Joern Toedling for developing a R code to evaluate Incucyte results and support throughout the project. We thank Filippos Klonomou for the Brunello plasmid pool sequence analysis, Kathy Astrahantseff for manuscript editing, Susan Cohn (University of Chicago) for providing the NBLW-R cell line and Louisa-Marie Krutzfeldt for data upload to the sequencing read archive (SRA). The authors thank the Genomics and Proteomics Core facilities at DKFZ for sequencing support.

Authors' contributions

M.B. and E.T. designed and conducted experiments, analyzed, interpreted, and visualized data, and wrote the manuscript. M.D. performed the read-out assay for perturbation experiments and performed modelling. A.W. and A.M.G. conducted experiments. M.Bo. contributed to the manuscript and performed computational analysis of CRISPR screen data. F.H. discussed results and experimental setup, reviewed, and edited the manuscript, supervised the project, and was involved in funding acquisition. E.R.F. analyzed LAN-5 sequencing data and visualized patient data. J.J.M., S.E. and K.O. conducted high-throughput drug screening experiments, analyzed the data, and discussed results. J.H.S. wrote and edited the manuscript, conceptualized, and supervised the project and acquired funding. C.K. co-supervised and conceptualized the project and reviewed the manuscript. A.G.H. and A.E. reviewed and edited the manuscript. N.B. discussed experiments and results, edited the manuscript. L.C., N.J., J.A., G.B., J.H.S. and M.F. designed and performed the clinical study. H.E.D., P.L. and A.K. were clinical partners (tumor sample acquisition). C.R. managed patient data at the university hospital cologne. N.J. managed patient data at GOSH. H.D.G. shared knowledge on CRISPR screening. P.C. performed ddPCR experiment. R.S. analysed the ctDNA for the GOSH patient. B.M.C., K.B., E.F., E.C., D.H., E.K., P.P. and M.H. were involved in clinical data acquisition or performed NGS panel sequencing. The author(s) read and approved the final manuscript.

Funding

Open Access funding enabled and organized by Projekt DEAL. Mareike Berlak is supported by the Berlin School of Integrative Oncology (BSIO). Elias Rodriguez-Fos is supported by the Alexander von Humboldt Foundation. Anton George Henssen is supported by the Deutsche Forschungsgemeinschaft (DFG, German Research Foundation)–398299703 and the European Research Council (ERC) under the European Union's Horizon 2020 research and innovation program (grant agreement No.949172). Annette Künkele is participant in the BIH-Charité Advanced Clinician Scientist Pilotprogram funded by the Charité –Universitätsmedizin Berlin and the Berlin Institute of Health. Johannes Hubertus Schulte has received funding from the Innovative Medicines Initiative 2 Joint Undertaking under grant agreement No 116064-ITCC-P4-H2020-JTI-IMI2–2015-07. We also received funding by the German Cancer Consortium (DKTK) for sequencing experiments. Mike Hubank, Paula Proszek and Paul Carter were supported by the National Institute for Health Research (NIHR) Biomedical Research Centre at The Royal Marsden NHS Foundation Trust and The Institute of Cancer Research, London. Reda Stankunaite was funded by Christopher's Smile. Deborah Hughes and Eleni Koutroumanidou were supported by Children with Cancer UK/Cancer Research UK SMPaeds (17–235/A24566). Louis Chesler was supported by the Institute of Cancer Research and The Higher Education Funding Council for England. Louis Chesler, Elizabeth Tucker, Barbara Martins da Costa, Karen Barker and Elicia Fyle were supported by the Cancer Research UK Programme Grant A28278. Elizabeth Calton was supported by Children with Cancer UK Clinical Research Fellowship – CWL022X. John Anderson was supported by the National Institute for Health Research (NIHR) Great Ormond Street Biomedical Research Centre. Neha Jain was supported by the Great Ormond Street Hospital Children's Charity Ollie Anstey Brighter Future Fund. The research group of Jan Jasper Molenaar was supported by the COMPASS consortium (Award No. ERAPERMED2018–121 within the ERAPerMed framework).

Availability of data and materials

The CRISPR-Cas9 knockout screen datasets analysed during the current study are available as FASTQ Files in the NCBI Sequence Read Archive (SRA) with the BioProject accession number PRJNA765129 and will be publicly available as of the date of publication (reviewer link: <https://dataview.ncbi.nlm.nih.gov/object/PRJNA765129?reviewer=s6aulos3t1j2qhp94f44u19fe8>).

The whole exome sequencing (WES) dataset for the LAN-5 cell line generated and analysed during the current study is available as FASTQ Files in the Sequence Read Archive (SRA) repository with the BioProject accession number PRJNA765501 (<https://www.ncbi.nlm.nih.gov/sra/?term=SRR16018268>). The panel sequencing dataset for the cell line SH-SY5Y generated and analysed during the current study is available as FASTQ Files in Sequence Read Archive (SRA) with the BioProject accession number PRJNA772100 (<https://www.ncbi.nlm.nih.gov/sra/?term=SRR16387283>).

The patient sequencing datasets of patients treated in Berlin are available in the European Genome-Phenome Archive (EGA) repository with the study number: EGAS00001005791 and dataset number: EGAD00001008343 (<https://ega-archive.org/datasets/EGAD00001008343>).

The patient sequencing datasets of the patient treated in London, UK are available in the European Genome-Phenome Archive (EGA) repository with the study numbers: EGAS00001006163 and EGAS00001006162. The patient sequencing datasets of the patient treated in Cologne, Germany used during the current study are available from the corresponding author on reasonable request. Cell lines generated in this study have not been deposited but are available upon request, with restrictions to the availability of the neuroblastoma cell line NBLW-R as the IP is held by The University of Chicago. Further information, incucyte images and requests for resources and reagents should be directed to and will be fulfilled by the corresponding author, Johannes Hubertus Schulte (johannes.schulte@charite.de or johannes.schulte@uni-due-de).

Declarations

Ethics approval and consent to participate

Patients from Berlin, Germany were 22 months (patient 1, female) and 3 months old (patient 2, male) at diagnosis. The patient from London, UK was 26 months old (patient 3, female) and the patient from Cologne, Germany (patient 4, male) was 14 months old at diagnosis. For further information see Fig. 5A. German patients had been enrolled in the German Neuroblastoma Registry (NB Registry 2016) (<https://kinderklinik.uk-koeln.de/forschung/onkologie/neuroblastom-studie/>). Written informed consent from patients or parents/guardians were obtained within the registry, ethics approval (16–432) was obtained from the ethics committee of the university hospital cologne. The GOSH patient was included in two research studies that had full UK research ethics approval and participated following informed consenting. Study one “Liquid biopsy study” was used for initial detection of mutations in plasma samples; study two “Strategic Medicine-Paediatrics” sequences tumour samples at time of relapse.

All in vivo experimental protocols were monitored and approved by the ICR Animal Welfare and Ethical Review Body, in compliance with guidelines specified by the UK Home Office Animals (Scientific procedures) Act 1986 and the United Kingdom National Cancer Research Institute Guidelines for the Welfare of Animals in Cancer Research [67].

Consent for publication

We obtained consent for publication of each patient parents or legal guardian.

Competing interests

The authors declare that they have no competing interests.

Author details

¹Department of Pediatric Oncology/Hematology, Charité – Universitätsmedizin Berlin, Augustenburger Platz 1, 13353 Berlin, Germany. ²Berlin School of Integrative Oncology (BSIO), Augustenburger Platz 1, 13353 Berlin, Germany. ³Department of Clinical Pharmacy and Biochemistry, Institute of Pharmacy, Freie Universität Berlin, Kelchstr.31, 12169 Berlin, Germany. ⁴Paediatric Solid Tumour Biology and Therapeutics Team, Clinical Division and Cancer Therapeutics Division, The Institute of Cancer Research, 15 Cotswold Road, Sutton, Surrey SM2 5NG, UK. ⁵Otto Warburg Laboratory Gene Regulation and Systems Biology of Cancer, Max Planck Institute for Molecular

Genetics, Berlin, Germany. ⁶Institute of Pathology, Charité-Universitätsmedizin Berlin, 10117 Berlin, Germany. ⁷IRI Life Sciences, Humboldt University Berlin, 10115 Berlin, Germany. ⁸Experimental and Clinical Research Center (ECRC) of the Charité and Max-Delbrück-Center for Molecular Medicine (MDC) in the Helmholtz Association, 13125 Berlin, Germany. ⁹Princess Maxima Center for Pediatric Oncology, Utrecht, The Netherlands. ¹⁰Molecular Diagnostics Department, The Institute of Cancer Research and Clinical Genomics, The Royal Marsden NHS Foundation, London, UK. ¹¹Cancer Section, UCL Great Ormond Street Institute of Child Health, London, UK. ¹²Department of Experimental Pediatric Oncology, Center for Molecular Medicine Cologne, 50931 Cologne, Germany. ¹³Department of pharmaceutical sciences, Utrecht University, Utrecht, The Netherlands. ¹⁴Department of Pediatric Hematology and Oncology, University Hospital, Tübingen, Germany. ¹⁵German Cancer Consortium (DKTK), Berlin, Germany. ¹⁶German Cancer Research Center (DKFZ), 69120 Heidelberg, Germany. ¹⁷Berlin Institute of Health (BIH) at Charité—Universitätsmedizin Berlin, 10117 Berlin, Germany. ¹⁸Medical Faculty, Martin Luther University Halle-Wittenberg, Halle (Saale), 06120 Halle, Germany.

Received: 9 January 2022 Accepted: 22 April 2022

Published online: 10 June 2022

References

- Bedard PL, Hyman DM, Davids MS, Siu LL. Small molecules, big impact: 20 years of targeted therapy in oncology. *Lancet*. 2020;395(10229):1078–88.
- Groenendijk FH, Bernards R. Drug resistance to targeted therapies: déjà vu all over again. *Mol Oncol*. 2014;8(6):1067–83.
- Ellis LM, Hicklin DJ. Resistance to targeted therapies: refining anti-cancer therapy in the era of molecular oncology. *Clin Cancer Res*. 2009;15(24):7471.
- Hutchison DJ. Cross resistance and collateral sensitivity studies in CANCER chemotherapy. *Adv Cancer Res*. 1963;7:235–50. [https://doi.org/10.1016/s0065-230x\(08\)60984-7](https://doi.org/10.1016/s0065-230x(08)60984-7).
- Nakamura S, Shiota M, Nakagawa A, Yatabe Y, Kojima M, Motoori T, et al. Anaplastic large cell lymphoma: a distinct molecular pathologic entity: a reappraisal with special reference to p80(NPM/ALK) expression. *Am J Surg Pathol*. 1997;21(12):1420–32.
- Soda M, Choi YL, Enomoto M, Takada S, Yamashita Y, Ishikawa S, et al. Identification of the transforming EML4-ALK fusion gene in non-small-cell lung cancer. *Nature*. 2007;448(7153):561–6.
- Coffin CM, Patel A, Perkins S, Elenitoba-Johnson KS, Perlman E, Griffin CA. ALK1 and p80 expression and chromosomal rearrangements involving 2p23 in inflammatory myofibroblastic tumor. *Mod Pathol*. 2001;14(6):569–76.
- Solomon B, Bauer TM, De Marinis F, Felip E, Goto Y, Liu G, et al. LBA2 Lorlatinib vs crizotinib in the first-line treatment of patients (pts) with advanced ALK-positive non-small cell lung cancer (NSCLC): results of the phase III CROWN study. *Ann Oncol*. 2020;31:51180–S1.
- Shaw AT, Bauer TM, de Marinis F, Felip E, Goto Y, Liu G, et al. First-line Lorlatinib or Crizotinib in advanced ALK-positive lung Cancer. *N Engl J Med*. 2020;383(21):2018–29.
- Smolle E, Taucher V, Lindenmann J, Jost PJ, Pichler M. Current knowledge about mechanisms of drug resistance against ALK inhibitors in non-small cell lung Cancer. *Cancers (Basel)*. 2021;13(4):1420–32.
- Brodeur GM. Neuroblastoma: biological insights into a clinical enigma. *Nat Rev Cancer*. 2003;3(3):203–16.
- Padovan-Merhar OM, Raman P, Ostrovnya I, Kalletla K, Rubnitz KR, Sanford EM, et al. Enrichment of targetable mutations in the relapsed neuroblastoma genome. *Proc Natl Acad Sci U S A*. 2016;113(12):e1006501.
- Schleiermacher G, Javanmardi N, Bernard V, Leroy Q, Cappo J, Rio Frio T, et al. Emergence of new ALK mutations at relapse of neuroblastoma. *J Clin Oncol*. 2014;32(25):2727–34.
- Carén H, Abel F, Kogner P, Martinsson T. High incidence of DNA mutations and gene amplifications of the ALK gene in advanced sporadic neuroblastoma tumours. *Biochem J*. 2008;416(2):153–9.
- Chen Y, Takita J, Choi YL, Kato M, Ohira M, Sanada M, et al. Oncogenic mutations of ALK kinase in neuroblastoma. *Nature*. 2008;455(7215):971–4.
- George RE, Sanda T, Hanna M, Fröhling S, Luther W 2nd, Zhang J, et al. Activating mutations in ALK provide a therapeutic target in neuroblastoma. *Nature*. 2008;455(7215):975–8.
- Janoueix-Lerosey I, Lequin D, Brugières L, Ribeiro A, de Pontual L, Combaret V, et al. Somatic and germline activating mutations of the ALK kinase receptor in neuroblastoma. *Nature*. 2008;455(7215):967–70.
- Mosse YP, Laudenslager M, Longo L, Cole KA, Wood A, Attiyeh EF, et al. Identification of ALK as a major familial neuroblastoma predisposition gene. *Nature*. 2008;455(7215):930–5.
- De Brouwer S, De Preter K, Kumps C, Zabrocki P, Porcu M, Westerhout EM, et al. Meta-analysis of neuroblastomas reveals a skewed ALK mutation spectrum in tumors with MYCN amplification. *Clin Cancer Res*. 2010;16(17):4353–62.
- Eleveld TF, Oldridge DA, Bernard V, Koster J, Colmet Daage L, Diskin SJ, et al. Relapsed neuroblastomas show frequent RAS-MAPK pathway mutations. *Nat Genet*. 2015;47(8):864–71.
- Heukamp LC, Thor T, Schramm A, De Preter K, Kumps C, De Wilde B, et al. Targeted expression of mutated ALK induces neuroblastoma in transgenic mice. *Sci Transl Med*. 2012;4(141):141ra91.
- Hallberg B, Palmer RH. Mechanistic insight into ALK receptor tyrosine kinase in human cancer biology. *Nat Rev Cancer*. 2013;13(10):685–700.
- Lambertz I, Kumps C, Claeys S, Lindner S, Beckers A, Janssens E, et al. Upregulation of MAPK negative feedback regulators and RET in mutant ALK neuroblastoma: implications for targeted treatment. *Clin Cancer Res*. 2015;21(14):3327–39.
- Emdal KB, Pedersen AK, Bekker-Jensen DB, Tsafou KP, Horn H, Lindner S, et al. Temporal proteomics of NGF-TrkA signaling identifies an inhibitory role for the E3 ligase Cbl-b in neuroblastoma cell differentiation. *Sci Signal*. 2015;8(374):ra40.
- Simon T, Hero B, Schulte JH, Deubzer H, Hundsdoerfer P, von Schweinitz D, et al. 2017 GPOH guidelines for diagnosis and treatment of patients with Neuroblastic tumors. *Klin Padiatr*. 2017;229(3):147–67.
- Bellini A, Pötschger U, Bernard V, Lapouble E, Baulande S, Ambros PF, et al. Frequency and prognostic impact of ALK amplifications and mutations in the European neuroblastoma study group (SIOPEN) high-risk neuroblastoma trial (HR-NBL1). *J Clin Oncol*. 2021;39(30):Jco2100086.
- Simon T, Berthold F, Borkhardt A, Kremens B, De Carolis B, Hero B. Treatment and outcomes of patients with relapsed, high-risk neuroblastoma: results of German trials. *Pediatr Blood Cancer*. 2011;56(4):578–83.
- Maris JM. Recent advances in neuroblastoma. *N Engl J Med*. 2010;362(23):2202–11.
- Cohn SL, Pearson AD, London WB, Monclair T, Ambros PF, Brodeur GM, et al. The international neuroblastoma risk group (INRG) classification system: an INRG task force report. *J Clin Oncol*. 2009;27(2):289–97.
- Foster JH, Voss SD, Hall DC, Minard CG, Balis FM, Wilner K, et al. Activity of Crizotinib in patients with ALK-aberrant relapsed/refractory neuroblastoma: a Children's oncology group study (ADVL0912). *Clin Cancer Res*. 2021;27:3543–8.
- Mossé YP, Lim MS, Voss SD, Wilner K, Ruffner K, Laliberte J, et al. Safety and activity of crizotinib for paediatric patients with refractory solid tumours or anaplastic large-cell lymphoma: a Children's oncology group phase 1 consortium study. *Lancet Oncol*. 2013;14(6):472–80.
- Fischer M, Moreno L, Ziegler DS, Marshall LV, Zwaan CM, Irwin M, et al. Ceritinib in paediatric patients with anaplastic lymphoma kinase-positive malignancies: an open-label, multicentre, phase 1, dose-escalation and dose-expansion study. *Lancet Oncol*. 2021;22(12):1764–76. [https://doi.org/10.1016/S1470-2045\(21\)00536-2](https://doi.org/10.1016/S1470-2045(21)00536-2). Epub 2021 Nov 12.
- Goldsmith KC, Kayser K, Groshen SG, Chioda M, Thurm HC, Chen J, et al. Phase I trial of lorlatinib in patients with ALK-driven refractory or relapsed neuroblastoma: a new approaches to neuroblastoma consortium study. *J Clin Oncol*. 2020;38(15_suppl):10504.
- Debruyne DN, Bhatnagar N, Sharma B, Luther W, Moore NF, Cheung NK, et al. ALK inhibitor resistance in ALK(F1174L)-driven neuroblastoma is associated with AXL activation and induction of EMT. *Oncogene*. 2016;35(28):3681–91.
- Debruyne DN, Dries R, Sengupta S, Seruggia D, Gao Y, Sharma B, et al. BORIS promotes chromatin regulatory interactions in treatment-resistant cancer cells. *Nature*. 2019;572(7771):676–80.
- Trigg RM, Lee LC, Prokoph N, Jahangiri L, Reynolds CP, Amos Burke GA, et al. The targetable kinase PIM1 drives ALK inhibitor resistance in high-risk neuroblastoma independent of MYCN status. *Nat Commun*. 2019;10(1):5428.

37. Doench JG, Fusi N, Sullender M, Hegde M, Vaimberg EW, Donovan KF, et al. Optimized sgRNA design to maximize activity and minimize off-target effects of CRISPR-Cas9. *Nat Biotechnol.* 2016;34(2):184–91.
38. Li W, Koster J, Xu H, Chen CH, Xiao T, Liu JS, et al. Quality control, modeling, and visualization of CRISPR screens with MAGeCK-VISPR. *Genome Biol.* 2015;16:281.
39. Sanson KR, Hanna RE, Hegde M, Donovan KF, Strand C, Sullender ME, et al. Optimized libraries for CRISPR-Cas9 genetic screens with multiple modalities. *Nat Commun.* 2018;9(1):5416.
40. Klinger B, Sieber A, Fritsche-Guenther R, Witzel F, Berry L, Schumacher D, et al. Network quantification of EGFR signaling unveils potential for targeted combination therapy. *Mol Syst Biol.* 2013;9:673.
41. Saez-Rodriguez J, Goldsipe A, Muhlich J, Alexopoulos LG, Millard B, Lauffenburger DA, et al. Flexible informatics for linking experimental data to mathematical models via DataRail. *Bioinformatics.* 2008;24(6):840–7.
42. Dorel M, Klinger B, Sieber A, Prahlad A, Gross T, Bosdriesz E, et al. Modelling signalling networks from perturbation data. *Bioinformatics.* 2018;34:4079–86.
43. Hecht M, Schulte JH, Eggert A, Wilting J, Schweigerer L. The neurotrophin receptor TrkB cooperates with c-met in enhancing neuroblastoma invasiveness. *Carcinogenesis.* 2005;26(12):2105–15.
44. Basu T, Gutmann D, Fletcher J, Glover T, Collins F, Downward J. Aberrant regulation of ras proteins in malignant tumour cells from type 1 neurofibromatosis patients. *Nature.* 1992;356:713–5.
45. Bollag G, Clapp D, Shih S, Adler F, Zhang Y, Thompson P, et al. Loss of NF1 results in activation of the Ras signaling pathway and leads to aberrant growth in haematopoietic cells. *Nat Genet.* 1996;12:144–8.
46. Simanshu DK, Nissley DV, McCormick F. RAS proteins and their regulators in human disease. *Cell.* 2017;170(1):17–33.
47. Der CJ, Finkel T, Cooper GM. Biological and biochemical properties of human rasH genes mutated at codon 61. *Cell.* 1986;44(1):167–76.
48. Temeles GL, Gibbs JB, D'Alonzo JS, Sigal IS, Scolnick EM. Yeast and mammalian ras proteins have conserved biochemical properties. *Nature.* 1985;313(6004):700–3.
49. Friday BB, Yu C, Dy GK, Smith PD, Wang L, Thibodeau SN, et al. BRAF V600E disrupts AZD6244-induced abrogation of negative feedback pathways between extracellular signal-regulated kinase and Raf proteins. *Cancer Res.* 2008;68(15):6145–53.
50. Fritsche-Guenther R, Witzel F, Sieber A, Herr R, Schmidt N, Braun S, et al. Strong negative feedback from Erk to Raf confers robustness to MAPK signalling. *Mol Syst Biol.* 2011;7:489.
51. Nahta R, Yu D, Hung MC, Hortobagyi GN, Esteva FJ. Mechanisms of disease: understanding resistance to HER2-targeted therapy in human breast cancer. *Nat Clin Pract Oncol.* 2006;3(5):269–80.
52. Rini BI, Atkins MB. Resistance to targeted therapy in renal-cell carcinoma. *Lancet Oncol.* 2009;10(10):992–1000.
53. Redaelli S, Ceccon M, Zappa M, Sharma GG, Mastini C, Mauri M, et al. Lorlatinib treatment elicits multiple on- and off-target mechanisms of resistance in ALK-driven Cancer. *Cancer Res.* 2018;78(24):6866–80.
54. Liu T, Mergerian MD, Rowe SP, Pratilas CA, Chen AR, Ladle BH. Exceptional response to the ALK and ROS1 inhibitor lorlatinib and subsequent mechanism of resistance in relapsed ALK F1174L-mutated neuroblastoma. *Cold Spring Harb Mol Case Stud.* 2021;7(4).
55. Kuenzi BM, Remsing Rix LL, Stewart PA, Fang B, Kinose F, Bryant AT, et al. Polypharmacology-based ceritinib repurposing using integrated functional proteomics. *Nat Chem Biol.* 2017;13(12):1222–31.
56. Holzel M, Huang S, Koster J, Ora I, Lakeman A, Caron H, et al. NF1 is a tumor suppressor in neuroblastoma that determines retinoic acid response and disease outcome. *Cell.* 2010;142(2):218–29.
57. Ackermann S, Cartolano M, Hero B, Welte A, Kahlert Y, Roderwieser A, et al. A mechanistic classification of clinical phenotypes in neuroblastoma. *Science.* 2018;362(6419):1165–70.
58. de Bruin EC, Cowell C, Warne PH, Jiang M, Saunders RE, Melnick MA, et al. Reduced NF1 expression confers resistance to EGFR inhibition in lung cancer. *Cancer Discov.* 2014;4(5):606–19.
59. Whittaker SR, Theurillat JP, Van Allen E, Wagle N, Hsiao J, Cowley GS, et al. A genome-scale RNA interference screen implicates NF1 loss in resistance to RAF inhibition. *Cancer Discov.* 2013;3(3):350–62.
60. Boettcher M, Tian R, Blau JA, Markegard E, Wagner RT, Wu D, et al. Dual gene activation and knockout screen reveals directional dependencies in genetic networks. *Nat Biotechnol.* 2018;36(2):170–8.
61. Pearson A, Proszek P, Pascual J, Fribbens C, Shamsher MK, Kingston B, et al. Inactivating. *Clin Cancer Res.* 2020;26(3):608–22.
62. Greger JG, Eastman SD, Zhang V, Bleam MR, Hughes AM, Smitheman KN, et al. Combinations of BRAF, MEK, and PI3K/mTOR inhibitors overcome acquired resistance to the BRAF inhibitor GSK2118436 Dabrafenib, mediated by NRAS or MEK mutations. *Mol Cancer Ther.* 2012;11:909–20.
63. Hintzsche J, Kim J, Yadav V, Amato C, Robinson SE, Seelenfreund E, et al. IMPACT: a whole-exome sequencing pipeline for integrating molecular profiles with actionable therapeutics in clinical samples. *J Am Med Inform Assoc.* 2016;23(4):721–30.
64. Ofir Dovrat T, Sokol E, Frampton G, Shachar E, Pelles S, Geva R, et al. Unusually long-term responses to vemurafenib in BRAF V600E mutated colon and thyroid cancers followed by the development of rare RAS activating mutations. *Cancer Biol Ther.* 2018;19(10):871–4.
65. Dorel M, Klinger B, Mari T, Toedling J, Blanc E, Messerschmidt C, et al. Neuroblastoma signalling models unveil combination therapies targeting feedback-mediated resistance. *PLoS Comput Biol.* 2021;17(11):e1009515. <https://doi.org/10.1371/journal.pcbi.1009515>.
66. Geoerger B, Moertel CL, Whitlock J, McCowage GB, Kieran MW, Bronsner A, et al. Phase 1 trial of trametinib alone and in combination with dabrafenib in children and adolescents with relapsed solid tumors or neurofibromatosis type 1 (NF1) progressive plexiform neurofibromas (PN). *J Clin Oncol.* 2018;36(15_suppl):10537.
67. Workman P, Aboagye EO, Balkwill F, Balmain A, Bruder G, Chaplin DJ, et al. Guidelines for the welfare and use of animals in cancer research. *Br J Cancer.* 2010;102(11):1555–77.

Publisher's Note

Springer Nature remains neutral with regard to jurisdictional claims in published maps and institutional affiliations.

Ready to submit your research? Choose BMC and benefit from:

- fast, convenient online submission
- thorough peer review by experienced researchers in your field
- rapid publication on acceptance
- support for research data, including large and complex data types
- gold Open Access which fosters wider collaboration and increased citations
- maximum visibility for your research: over 100M website views per year

At BMC, research is always in progress.

Learn more biomedcentral.com/submissions

